The Iranian Journal of Mechanical Engineering Transactions of ISME
Journal homepage: https://jmee.isme.ir/
Vol. 24, No. 1, 2023, pp. 15-39

Research Paper

DOI: https://doi.org/10.30506/jmee.2023.523710.1252
DOR: https://dorl.net/dor/20.1001.1.16059727.2023.24.1.2.6

Effects of Bronze Element Surface on Bubble Departure Size in Pool Boiling and its Prediction through ANN and GA Approaches

Masoud Rafiee*
Ph.D. Candidate

Akbar Mohammadidoust†
Assistant Professor

Mohsen Khooshehchin‡
Ph.D.

Samira Ghotbinasab§
M.Sc.

The present study investigates the surface roughness of the Bronze element on heat transfer in pool boiling process. The experiments were carried out with a solution of deionezed water (50%) and isopropanol (50%) in a specified container containing a hollow cylinder of bronze metal. The results indicated that the roughness index had a significant effect on the bubble dynamic. Increasing the surface roughness led to promote the bubble generation points and bubble departure diameter subsequently heat transfer enhancement through fluctuations in the solution. In addition, artificial neural network (ANN) and genetic algorithm (GA) were applied for developing the bubble departure diameter that the roughness index was one of the independent variables. Although the ANN was more capable than GA in data prediction, the GA could be employed as a more efficient and easy available approach. Therefore, the both models were powerful with acceptable errors (R2ANN=0.9982, R2GA =0.9929). Finally, the processed models were compared to Cole, Van Stralen, Lee and Stephane models. The results depicted that the ANN and GA methods had superior agreement with the experimental data than other models.

Keywords: Pool boiling, Bubble departure diameter, Surface roughness, Artificial neural network, Genetic algorithm

---

* Ph.D. Candidate, Department of Chemical Engineering, Mahshahr Branch, Islamic Azad University, Mahshahr, Iran, rafiee.chemengineer@gmail.com
† Corresponding Author, Assistant Professor, Department of Chemical Engineering, Kermanshah Branch, Islamic Azad University, Kermanshah, Iran, mohammadidoust@gmail.com, mohammadidoust@iauksh.ac.ir
‡ Ph.D., Department of Chemical Engineering, Kermanshah Branch, Islamic Azad University, Kermanshah, Iran, mohsen.khooshehchin@yahoo.com
§ M.Sc., Department of Chemical Industry, University of Applied and Technology, Center Dehloran, Iran, samiraghotbinasab@yahoo.com

Received: 2021/01/24, Revised: 2022/12/07, Accepted: 2023/10/04

1 Introduction

Increasing the energy demandled tooptimize the use of resources and avoiding its loss in the industries. In the oil, gas and petrochemical industries, a large amount of the energy is requireddue to heatingsystems such as heat exchangers. Operational parameters including geometry, material, element orientation and the heat transfer surface and so oncan play significant roles in increasing the heat transfer at an optimum level. Therefore, it is essential to determine a way to increase energy transfer in the processes. Pool boiling as one of the important methods in transferring heat has widely been employed. Despite careful studies and investigating the significant effects of the parameters on the heat transfer, the effects of the heat transfer surface has not precisely been discussed [1].

In the pool boiling, heat transfer surface is a prominent parameter in producing bubbles and their circulationwhich caused to turbulency in the solution, subsequently promotion of the boiling heat transfer coefficient (BHTC). Bubble production is related to the properties of the boiling fluid and heat transfer surface. Material, orientation, geometry, and physical properties of the surface are considred to study bubble production. To improve of fluid properties, adding nanoparticles into fluid have been studied in order to increase the BHTC in many resereches [2-11]. In addition, the creation of microfine-pin [12-14], microgrooves and microcavities [15, 16] and Roughness [17-19] on the heat transfer surface have been performed to enhance the BHTC.

Researchers have classified developed surfaces into two categories, namely structured and porous surfaces [20-25]. Porous coatings can be created by techniques such as plasma spraying, flame spraying, electro-depositioning and sintering [26]. The effect of roughness parameters on increasing BHTC in nucleate boiling has been recognized since 2012. Jakob observed that increasing the BHTC of water on a grooved surface is about three times greater than a simple surface [27]. The surface roughness can have a profound effect on heat transfer in single-phase and two-phase convection processes from the surface of the metal to the fluid [28].

Martou and Rohsenow [29] found that the surface roughness had a significant effect on the amount of heat flux and the BHTC during the fluid boiling process and even before it. It is possible to increase the roughness of the heat transfer surface by sandblasting, chemical etching and creating several artificial cavities [13].

Increasing the number of active sites of bubble nucleation in the heat transfer surface is one of the main reasons for the increase of the BHTC on rough surfaces [30-34]. In addition, the effects of roughness on different types of surfaces (i.g. flat and tubular) have been studied in nucleate boiling. In the meantime, tubular surfaces that are widely used in fluid transfer have been studied many times [35-39]. Moreover, the surface roughness in vertical tubes acted better than horizontal ones [36-38]. Recently, usingthe combination of different conditions in surface design; i.g. simultaneous monitoring of wettability and surface roughness, which is one of the techniques for the surface modification, has attracted attention of researchers [30]. The bubble departure diameter is well established as an important parameter for determining the heat transfer rate during the boiling process[40-42]. In the past decades, a number of empirical and semi-experimental methods have been proposed to predict the bubble departure diameter in pool boiling [14, 37, 43-56].

Some models are presented in Table (1). The error of the output and compiexity of the methods led to find a precise model for predicting the buble departure diameter in pool boiling. In this study the effects of severalroughnesses of bronze surface on the growth and production of the bubbles in a water-isopropanol solution were investigated. Furthermore, two novel numerical models were processed through artificial neural network (ANN) and genetic algorithm (GA) in order to exact predicts the bubble departure diameter. Finally, these models were comparedwith other models.

Table 1 The proposed relations of the researchers to the bubble diameters

Reference	Correlation	Limitation
Zhou 2018[14]	$D_d = 0.08Ja^{0.6}\sqrt{\frac{2\delta}{g(\rho_l - \rho_{v)}}}$	Small diameter function
Fritz 1935 [44]	$D_d = 0.0146\beta\,[\frac{2g_c\,\sigma}{g\,(\rho_L - \rho_v)}]^{1/2}$ β=Contact angel for water 48 C_d=0.0148 for water	Pure liquids and multi-component solutions
Ruckenstei 1964[45]	$D_d = \left[\frac{3\pi^2\rho_L\alpha^2 g^{0.5}(\rho_L - \rho_g)}{\sigma^{1.5}}\right]Ja^{\frac{4}{3}}\sqrt{\frac{2\sigma}{g(\rho_L - \rho_v)}}$	Pure liquids and multi-component solutions
Cole 1967[46]	$D_d = 0.04Ja[\frac{2\sigma}{g\left(\rho_L - \rho_g\right)}]^{1/2}$	Pure liquids and multi-component solutions
Van stralen 1978[57]	$D_d = 2.63[\frac{Ja^2\alpha^2}{g}]^{\frac{1}{3}}[1 + \left(\frac{2\pi}{3ja}\right)^{\frac{1}{2}}]^{\frac{1}{4}}$	Pure liquids and multi-component solutions
Kutateladze, and Gogonin 1979[58]	$D_d = 0.25\sqrt{\frac{\sigma}{g(\rho_L - \rho_v)}}\left[1 + (\frac{Ja}{Pr}^2)\frac{1}{Ar}\right]^{\frac{1}{2}}$	----------
Kocamustafaogullari 1983[49]	$D_d = 2.64\times10^{-5}(\frac{\sigma}{g(\rho_L - \rho_v)})^{0.5}(\frac{(\rho_L - \rho_v)}{\rho_v})^{0.9}$	Pure liquid, high pressure range
Jensen and Memmel 1986[59]	$D_d = 2.97\times10^4\left(\frac{\rho}{\rho_{cr}}\right)^{-1.09}\left(\frac{K.T}{\rho_{cr}M}\right)^{\frac{1}{3}}$ $K_L = \left(\frac{Ja}{pr}\right)^2\left[\left[\frac{g\left(\rho_L - \rho_g\right)}{\mu_L^2}\right]\left[\frac{\sigma}{g(\rho_L - \rho_v)}\right]^{\frac{3}{2}}\right]^{-1}$ K=1.36×10^{-32} Boltzman constant M=molecular weight, ρ_{cr}=Critical point	------------
Gorenflo 1986[60]	$D_d = C\left(\frac{Ja^4\sigma_l{}^2}{g}\right)^{\frac{1}{3}}\left[1 + \left(1 + \frac{2\pi}{3Ja}\right)^{\frac{1}{2}}\right]^{\frac{4}{3}}$	C= 2.78 for propan C= 14.7 for R12 C= 16 for R22
Lee 2003[61]	$D_d = 2\left(\frac{25}{2}\sqrt{27} * Ja\left(\frac{\rho_l}{\sigma}\right)^{0.5}\right)^2$	Pure liquids and multi-component solutions
Balakrishnan, Sateesh 2005[53]	$D_d = \sqrt{\frac{12.N.\sigma}{M.g(\rho_L - \rho_v)}}$ $N = \frac{\sin\theta_m(1 - \cos\theta_m)}{\pi - \theta_m + \sin\theta_m\cos\theta_m}$ $M = \frac{(1 + \cos\theta_m)^2\,(2 - \cos\theta_m)}{\pi - \theta_m + \sin\theta_m\cos\theta_m}$	Pure liquids and multi-component solutions, on the vertical surfaces

Alvi Fazle 2010[62]	$D_d = mN_{Ca}{}^{n}(\frac{\sigma}{g(\rho\iota - \rho v)})^{0.5}$ m =40 and 0.33n= 0.33	Electrolyte solution
Phan 2009[56]	$D_d = 0.626977 * \frac{(2+3\cos\theta - cos^3\theta)}{4}(\frac{\delta}{g(\rho_l - \rho_v)})^{1/2}$	Correction of Fritz relation with energy factor θ≤90
Phan 2010[56]	$D_d = \left(6\sqrt{\frac{3}{2}}\right)^{\frac{1}{3}}\left(\frac{\rho_l}{\rho_v}\right)^{-\frac{1}{2}}(\frac{\rho_l}{\rho_v} - 1)^{1/3}\tan\theta^{-1/6} L_c$	Angle contact function, maximum volume, balance of forces $0 < \theta < 90$
Stephane 1992[63]	$\mathrm{D_d} = 0.25[1 + \left(\frac{\mathrm{Ja}}{\mathrm{Pr}}\right)^2 \frac{100000}{\mathrm{Ar}}]^{0.5}\sqrt{\frac{2\sigma}{g(\rho_L - \rho_g)}}$	Pure liquids and multi-component solutions
Cooper 1969[64]	$\mathrm{D_d} = \frac{4K_L\Delta T_{sat}}{\rho_l h_{fg}\sqrt{C\alpha}} tg^{\frac{1}{2}}$ C=0.64 Pr	Non-ionic solutions
Stanizowsk 1959[65]	$\mathrm{D_d} = 0.0071\left(\frac{2\sigma}{g(\rho_L - \rho_v)}\right)^{\frac{1}{2}}\left(1 + 0.435\frac{dD}{dt}\right)$	Pure liquids and multi-component solutions, Along with the time limits
Zuber 1962[66]	$D_b = \frac{4b}{\sqrt{\pi}} Ja\sqrt{\alpha_l}t$ b=1.73	…………..
Hatton and Hall 1966 [67]	$\mathrm{D_d^3}\frac{(\rho_L - \rho_v)}{\sigma} = \frac{164x^4}{g}\left(\frac{D_c\rho_L}{8} - \frac{\rho_L}{12} + \frac{\rho_v}{6}\right) - \frac{\sigma}{g}(\frac{D_c^2}{D_d} - D_c \sin\phi)$ $X = \frac{\sqrt{3}K\Delta T_{sat}}{H_{fg}f_g\sqrt{\pi\alpha}} D_c = \frac{4\sigma T_{sat}}{\rho_v H_{fg}(T_w - T_{sat})}$ /K = Boltzman Constant Φ =Angle	Pure liquids and multi-component solutions,Critical Diameter Function
Cole and Shulman 1966 [68]	$\mathrm{D_d} = 0.0208\phi\left[\frac{\sigma}{g(\rho_L - \rho_v)}\right]^{\frac{1}{2}}\left[1 + 0.0025\left(\frac{dD}{dt}\right)^{\frac{3}{2}}\right]$ $\Phi = \sqrt{3}$،$1$and$\frac{\pi}{2}$	----
Cole and Rohsenow 1966[69]	$\mathrm{D_d} = \mathrm{C.Ja}^{\frac{5}{4}}(\frac{\sigma}{g(\rho_L - \rho_v)})^{\frac{1}{2}}$ $\mathrm{C} = 1.5 \times 10^{-4}$for water	Pure liquids and multi-component solutions
Kweon 2000[70]	$\mathrm{D} = C_1(\frac{6\sigma\sin^2\phi}{g(\rho_L - \rho_v)Ke})$ $\mathrm{Ke} = 1 + C_2\left(\xi_v\xi_g/\Delta\rho\,.\,g\right)[(1 - \xi_v)\,/\,(1 + 2\xi)]^2$ ξ_v And ξ_g=Values to calculate the effect of the electric field	There is an electric field
Jamialamadi 2004[71]	$D_d = \frac{1}{96.75 + \frac{0.01425(\frac{q}{A})}{Ln(\frac{q}{A})}}$	Electrolyte solution

2 Experimental

2.1 Experimental set up and analyses

The apparatus used in this laboratory test was a 3-liter glass includingdeionized water (50%) and isopropanol (50%), as base solution. As shown in Figure (1), a hollow cylinder of bronze metal with an outer diameter of 24 mm, an internal diameter of 13 mm and a length of 210 mm wereconsidered as an element (heater) in the lower and middle part of this container. The high-thermal insulation glass has a thickness, length, width and height of 10 mm, 220 mm, 180 mm and 220 mm, respectively. To prevent heat loss, the aquarium surfaces was insulated with glass wool. A pencil bulb with a diameter of 11 mm, a length of 190 mm and a maximum power of 1 kW was employed in the middle of the element to generate heat. The bulb was powered by an electric power source that used to change the input voltage and record in the range of 0-240 V at 1 kW. A multi-meter in the range of 1 mV ~ 1 kV and 0.1 μA ~ 20 A used to measure the voltage and ampere consumption. As seen in Figure (2), to accurately record the temperature variations in the element surface by varying the voltage, three thermocouples (Alumel-chromel (K) type with a sensor length of 50 mm, a diameter of 2 mm, a range of 180 °C to 750 °C) were placed in three holes in the cross section of the elementwith an angle of 120°. The diameter and depth of the holes were 2 mm and 50 mm, respectively. To prevent the presence of air in the holes of the thermocouple sensors, silicon thermal paste used with a conductivity of 4 $W.m^{-1}.°C^{-1}$. To keep the volume of boiling solution and to check the parameters in the same conditions, a condenser was used at the top of the aquarium. There was a fourth thermocouple, whenthe solution temperature was deviated from its boiling temperature; an auxiliary element with a capacity of 1000W used in the container. In each step of the experiment, using the Sony PMW-300K1 high-speed camcorder, the changes in the heat transfer surface and boiling solution were recorded. The film was analyzed using the EDIUS software so that the bubble dynamic variations, including the bubble departing frequency, the average of a certain diameter of the output bubble and the density of the bubble nucleation site were determined. The experiments were performed at different roughnessescreated by sanding with numbers of 80, 180, 240, and 400. Roughness tester RT-620 was used to measure the surface roughness.

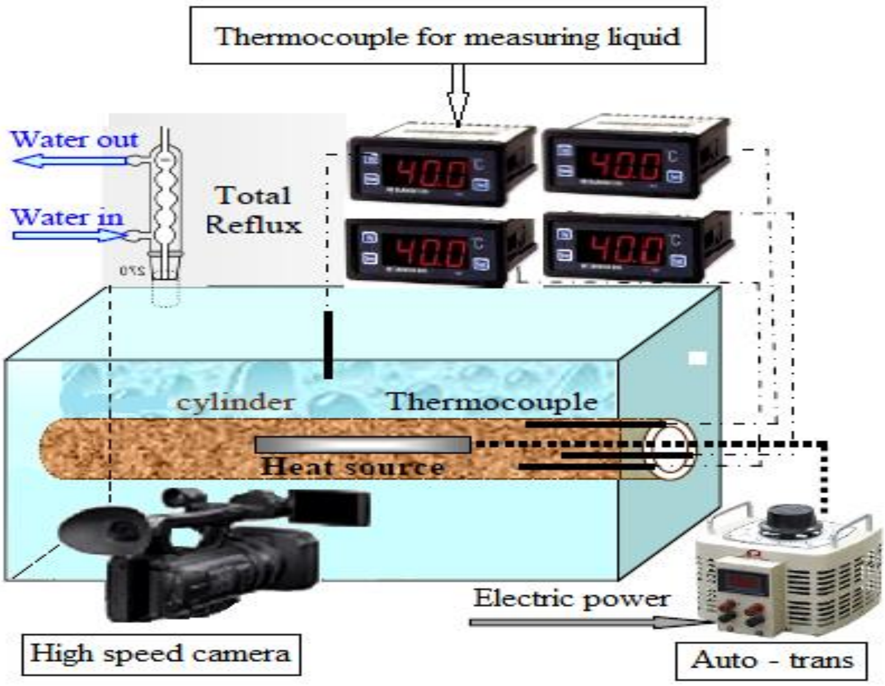

Figure 1 A schematic of the experimental apparatus

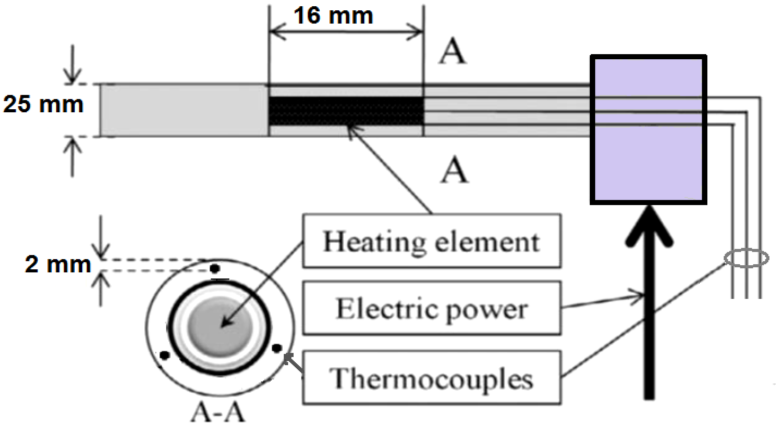

Figure 2 Some details of the heat rod

2.2 Material

In order to the preparation of the solutions, the dilution process was implemented by deionized water to the desired initial concentrations of isopropanol. The isopropanol was supplied from Merck, Inc., of the AR grade.

2.3 Experimental procedure

The experiments were donebythe isopropanol (50%) and deionzed water (50%)as base solution at volume of 1-liter. After the solution boiling by the auxiliary element, it was turned off and the pencil lamp inside of the bronze cylinder turned on to continue the boiling process. In saturated state, the solution was remained at its saturated temperature for 60 min. This opportunity led to eliminate air bubbles in the liquid phase and heater surface.
Thebubble departure diameter, active nucleation sites density and the BHTC were determined with 0.35, 0.92, 1.09 and 1.25 μm of surface roughness. The parameters were examined at eight heat fluxes. It should be noted that each test was repeated three times and the mean of the experimental data was considered.

3 Uncertainty and data reduction

The uncertainty of heat transfer coefficient can be estimated by the Newton cooling law:

$$h = \frac{q/A}{(T_S - T_{sat})} \tag{1}$$

Heat flux was calculated by the following equation:

$$\frac{q}{A} = \frac{(V.I)}{A.Cos\varphi} \tag{2}$$

The $\cos\varphi$was assumes to be equal to unity, because of the linear shape of heater section and the absent of any solenoid effect. The maximum estimated uncertainty of heat flux would be based on Equation (3) [37]:

$$\frac{\delta(q/A)}{q/A} = \sqrt{(\frac{\delta I}{I})^2 + (\frac{\delta V}{V})^2} \tag{3}$$

Before estimating the uncertainty for heat transfer coefficient, δh , it is necessary to estimate the uncertainty of temperature difference, $\delta\Delta T$ as follows [37]:

$$\delta\Delta T = \sqrt{(\delta T_S)^2 - (\delta T_{th})^2} \tag{4}$$

$$\frac{\delta h}{h} = \sqrt{(\frac{\delta I}{I})^2 + (\frac{\delta V}{V})^2 + (\frac{\delta T}{T})^2} \tag{5}$$

Since the exact recording of the heater surface temperature by thermocouple is important for analyzing the results and, on the other hand, the places of the thermocouples' installation are in small distance from the outer surface of the heater and this small spacing causes trivial difference in recording the real temperature, Equation (6) is used to correct this temperature error:

$$T_S = T_{th} - \frac{q'' b_s}{K_S} \tag{6}$$

Where, $b_s$is the distance between the thermocouple locations and the heat transfer surface and K_s is the thermal conductivity of the heatermaterial.
The average temperature of three thermocouples ($\overline{T_S}$)is calculated from the equation (7):

$$\overline{T}_S = \frac{1}{n}\sum_{i=1}^{n} T_{S.i} \tag{7}$$

The accuracies of the present uncertainty analysis for the experiments are tabulated in Table (2).

4 Modeling

Modeling is a powerful tool that can aid to fast predict of process response. It can be effective in decreasing the number of experiments and following the cost and time. In this study, the bubble departure diameter was considered the output of the process. The surface roughness is one of the independent variables that affectonthe bubble departure diameter.

Table 2 Uncertainty sources

Parameter	**Uncertainty**
Tube diameter	±0.01 mm
Tube length	±0.01 mm
Thermocouple, K-type	±0.1 °C
Voltage (V)	±1 V
Current (A)	±0.1 A
roughness measuring	±(0.07-0.10) µm
maximum heat flux of 76 kW m^{-2}	±1.8545 kW. m^{-2}

To exact evaluation, heat flux, temperature variations, density (liquid and vapor), thermal conductivity, entalphy, surface tension, heat capacity and dynamic viscosity were also accounted [49, 52, 59, 72, 73]. First, an artificial neural network was processed. Second, according to the parameters mentioned above and power-law equation, a GA based correlation was presented. Finally, the both models were compared to other models in the literature.

4.1 Artificial Neural Network

The artificial intelligence can estimate and realize the complex processes such as non-linear processes. The ANNs as one of the subsets of artificial intelligence are able to predict processes that lack simple and clear mathematical models. In this work, The MATLAB software (R2014a) was employed to model the buuble departure diameter on the bronze surface with different roughnesses. In general, The ANN including three layes namely input, hidden and output. Neurons play significan role in calculating and forecasting response(s). The neurons of each layer are connected by the sepecified layers and a continuous group was made by the weights and biases. Then, a logical pattern between inputs and outputs was made due to weights and biases. It follows the equation below:

$$Y_j = f_t\left(\sum_{i=1}^{n} w_{ji} x_i + b_j\right) \tag{8}$$

Where, $Y_j$is the output of jth neuron, w_{ji} is weight of jth neuron ith input, x_i is the independent variable, b_j is the jth neuron bias, n is number of input variables to jth neuron and f_t is the transfer function. There are different transfer functions in the ANN. “Tansig”, “Purelin” and “Logsig” are the conventional functions which used in the ANNs. The number of input and output variables determines the number of neurons in the input and output layers. For the hidden layer, optimizing the number of neurons is an appropriate criterion to achieve the minimum error[74].

The ANN including several network types as Feed-forward back propagation, Elman back propagation, Cascade-forward back propagation, Competitive, etc. In this work, the feed-forward back propagation was employed with a high accuracy compared with the others.

However, despite of powerful precision, the ANN models cannot prepare anobvious relationship among the effective parameters. In addition, a major lack of the neural networks is that the related physical processes are not easily comprehendedwhile statistical models can clear the variations of the process, obviously [74]. In this work, heat flux, roughness index, temperature variations, liquid density, vapor density, thermal conductivity of liquid, enthalpy, surface tension, heat capacity and dynamic viscosity of liquid as input variables and the bubble departure diameter as output response were considered. In addition, the feed-forward back propagationtype, transfer functions of “Tansig” (hidden layer) and “Purelin” (output layer) wereemployed with a lowest error compared to the others.

Table (3) reports the range of data points in training the ANN.

4.2 Genetic Algorithm

Genetic algorithm (GA) is the othersubset of the artificial intelligence and is a numerical solution for finding optimum response (maximum or minimum) in non-linear problems, especially. In general, GA makes a faster movement to find probability solutions in problem space. Desired responces are randomly attained and without expanding all the cases. GA is a special type of evolution algorithm that uses the biological techniques such as inheritance and mutation. It was first introduced by John Henry Holland [75].

Table 3 The range of data used in ANN training

Parameter	Type	Min	Max
q''	input	2754.498	71300.49
R_a	input	4.55E-07	0.000032
ΔT_{exp}	input	3.0178	21.966
$\rho_{l.mix}$	input	928.8603	937.5082
$\rho_{v.mix}$	input	2.5573	2.6433
$k_{l.mix}$	input	0.5500	0.5547
$h_{fg.mix}$	input	17388854	17668889
σ_{mix}	input	0.032312	0.034061
$C_{pl.mix}$	input	4079.488	4115.129
$\mu_{l.mix}$	input	0.000286	0.000333
D_b	output	0.00068	0.001414

In fact, GA uses Darwin's natural selection principles to find the optimal formula and matching with the desired pattern. It is often a good tool for regression-based prediction techniques.GA is a population through search algorithm thatuses the concept of reachingthe optimal one. The new populations are generated by repetitivegenetic operators on unit element in the population. The important items in the GA include the chromosome representation, selection, crossover, mutation, and fitness function[76]. Its procedure is as; a population of some chromosomes isset at the starting position, randomly. The fitness of each chromosome in the populationis estimated. Two chromosomes are chosen from the population regarding to the fitness value. The single-point crossover with crossover probability is employed on the both chromosometogenerate an offspring. Subsequently, uniform mutation operator is employed on generated offspring with mutation probability to generate a new offspring. It is put in new population. Finally, the selection, crossover, and mutation operations will be reiterated on this population until the new populationis achieved [75, 76]. In summary, in mathematical procedure, the GA includes objective function and constrains [65]. Optimum point is found based on them that can be extremum of the process. In addition, constrains are introducd according the related conditions. In engineering problems, related process and its conditions are the determiner of constrains. The GA through biological pattern searches the optimum point by several ways. Finally, outputs are attained after few times because calculations'rate of the software, artificial intelligence approaches [76]. According to the experimental results, a correlation among the buuble departure diameter (D_b) and heat flux (q''), roughness index (R_a), temperature variations(ΔT_{exp}), liquid density ($\rho_{l.mix}$), vapor density ($\rho_{v.mix}$), thermal conductivity of liquid ($k_{l.mix}$), enthalpy ($h_{fg.mix}$), surface tension (σ_{mix}), heat capacity($C_{pl.mix}$) and dynamic viscosity of liquid ($\mu_{l.mix}$) is attained by GA optimizer. A power-lawfunction is assumed as follows:

$$D_b = q''^{g_1} R_a{}^{g_2} \Delta T_{exp}{}^{g_3} \rho_{l.mix}{}^{g_4} \rho_{v.mix}{}^{g_5} k_{l.mix}{}^{g_6} h_{fg.mix}{}^{g_7} \sigma_{mix}{}^{g_8} C_{p,l.mix}{}^{g_9} \mu_{l.mix}{}^{g_{10}} \quad (9)$$

In this study, the optimum constant values (g_i) are determined through the experimental variables based on GA. Desired GA of the work was obtained by MATLAB software (R2014a).

5 Results and discussion

5.1 Experimental

First, to verify the functionality and accuracy of the laboratory apparatusbefore starting the data gathering, several tests were performedby deionized water as the base fluid. Then the results were compared with the three popular models of Gorenflo[51],Stephan[72], and Cooper [73]and these results were shown in Figure (3). As demonstrated in the figure, there is a superior agreement between the experimental data (three repetitions) and other models. In the present study, the element roughness effects on bubble growth changes were investigated. In addition, for a more detailed analysis, the density of nucleate sites and changes on the HTC were examined. In general, the purpose of examining the variations and behavior of the bubble departure diameter is to achieve a fluctuation state in its boiling solution. It is one of the influential factors in the HTC increase in pool boiling. It should be noted that a roughness should be selected as the base roughness to study the effective parameters in the boiling. The base roughness of the bronze element was chosen by 0.35 μm.

5. 1. 1 The roughness effect on the density of the bubble generator points

To investigate the effect of the heat transfer surface roughness on the density of the bubble generator points, four roughnesses of 0.35, 0.92, 1.09 and 1.25 μm were studied. It shoud be noted that attempts to increase the roughness uniformly were not possible due to an error. As shown in Figure (4), an increase in the roughness has raised the density of the bubble points onthe bronze element, which indicates an important and direct effect of the roughness on increasing the density of the bubble points. Moreover, the thermal conductivity of the element is other factor in promoting the density of the bubble points. The figure illustratesthat the increase in the heat flux led to increase the density at a constant roughness which more enhanhcement was observed in the rangeof 32-52 kW.m^{-2}. This can be explained that in high heat fluxes, a source with more energy transfer causes the nearby deactivated springs to be active through micolayers of vapor streams.

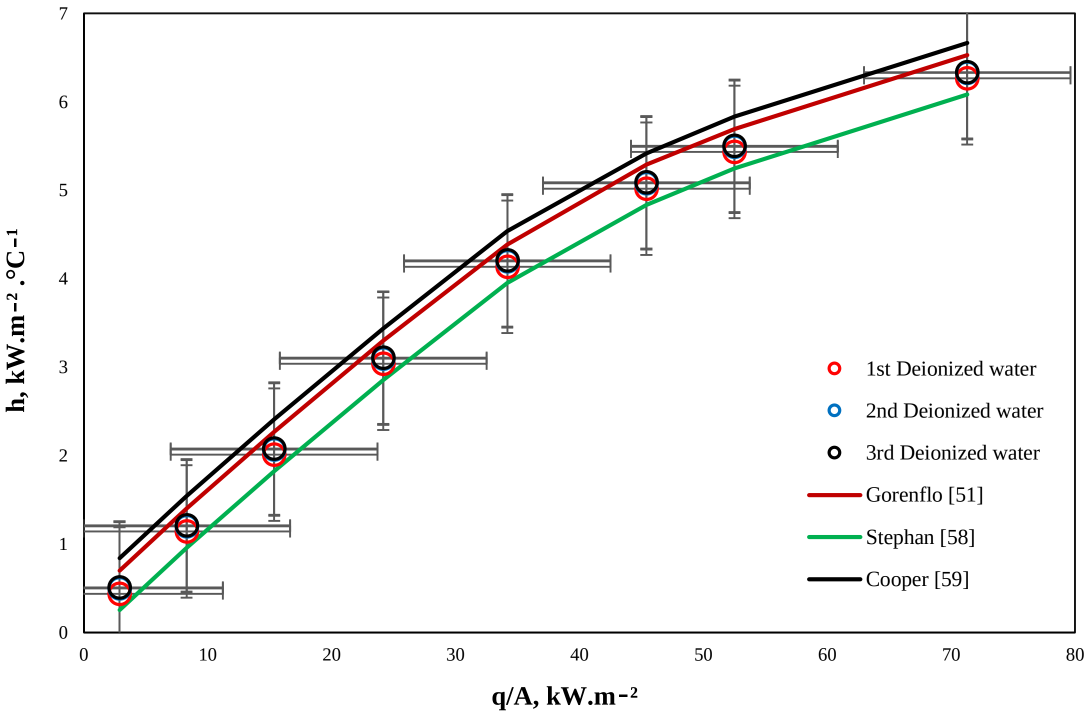

Figure 3 The comparison of the experimental results with the conventional models

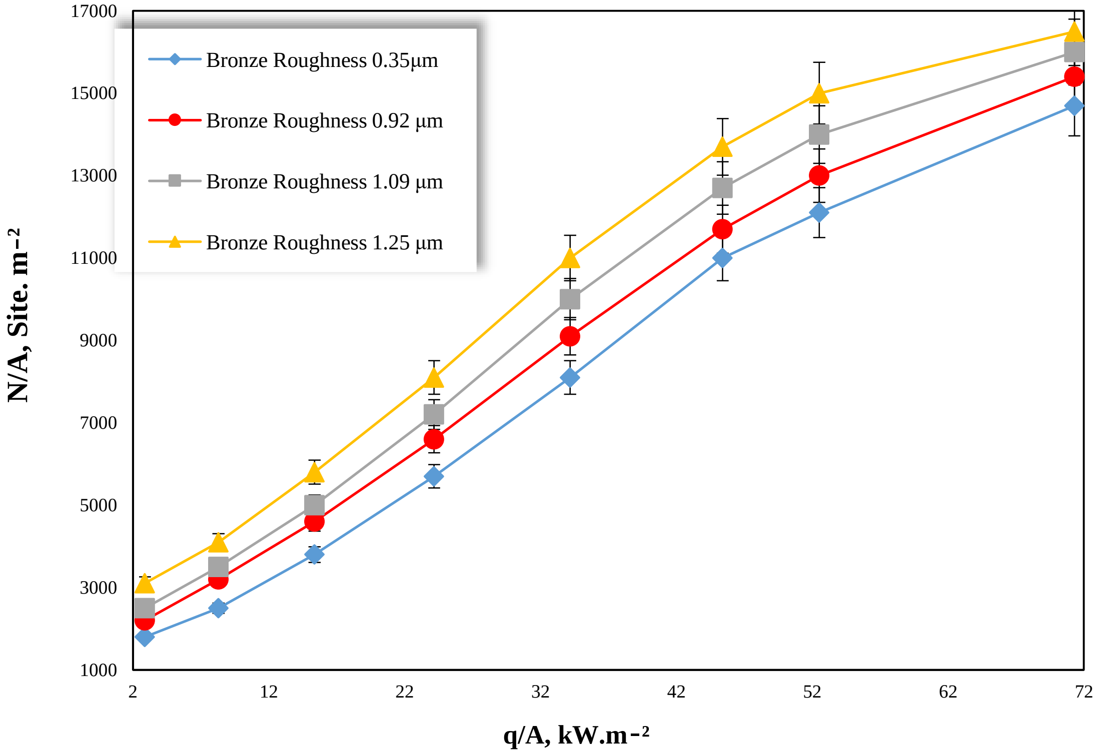

Figure 4 The effect of roughness on the density of the bubble generator points

5. 1. 2 The roughness effect on the bubble departure diameter

In the experimental study, the effects of roughness of bronze surface on the bubble departure diameterat 0.35, 0.92, 1.09 and 1.25 μm of surface roughness were investigated. Figure (5) shows the variations of the bubble diameter at different roughnesses. It can be seen in the figure that increasingthe surface roughness enhanced the bubble departure diameter at different heat fluxes. In addition, bubble diameter enhancement had a significant effect on the heat transfer. Although the increase of the bubble departure diameter can be attributed to the effect of the thermal conductivity, increasing the roughness and consequently, increasing the density of the bubble generator points causethe springs to come together to form a larger bubble. The largest increase in the bubble departure diameter occurred in the same range of 32-52 $kW.m^{-2}$ of the heat fluxcompred to earlier. It indicated the role of bubble generator points in increasing the bubble departure diameter.

5.1.3 The roughness effect on the boiling heat transfer coefficient

Increasing the roughness resulted in an increase in the density and diameter of the bubbles. In the following, the effect of the increase of the roughness on the BHTC was examined. As demonstrated in Figure (6), the surface with a high roughness has a high BHTC. This increase in the BHTC is madedue to an increase in the mixing and fluctuating the bubbles in boiling solution. In general, the higher density of the bubble generator points on the heat transfer surface led to the more generated bubbles resulted in more disturbances in the solution. On the other hand, the produced bubbles in the heat transfer surface with increasing the bubble departure diameter and subsequently moving inside the solutioncould create more disturbances than the smaller bubbles. Finally, the roughness index as a significant paramere can be considerd in promoting the bubble density, bubble diameter and following the BHTC. Figure (7) reveals a real image of the variations versus different roughnesses. The increase of the BHTC was about 36.5% for a bronze element with roughness between 0.35 and 1.25 μm.

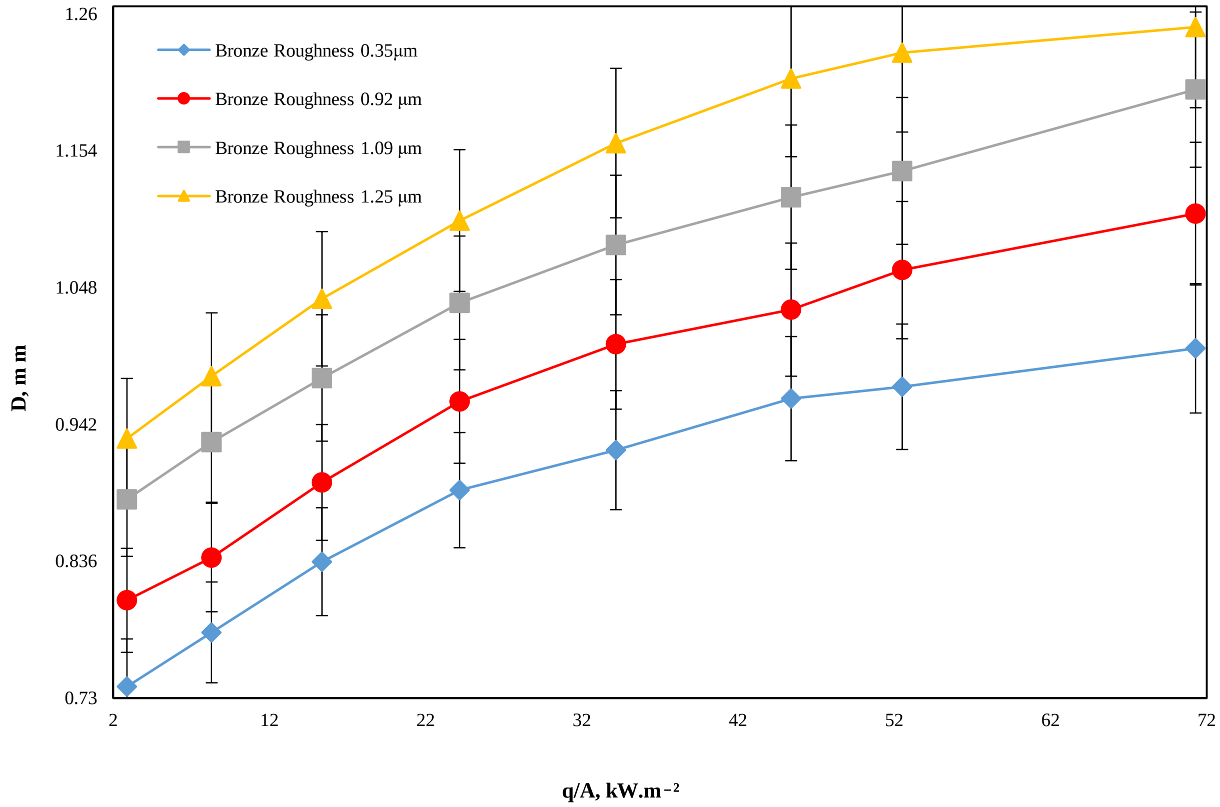

Figure 5 The effect of roughness on the bubble departure diameter

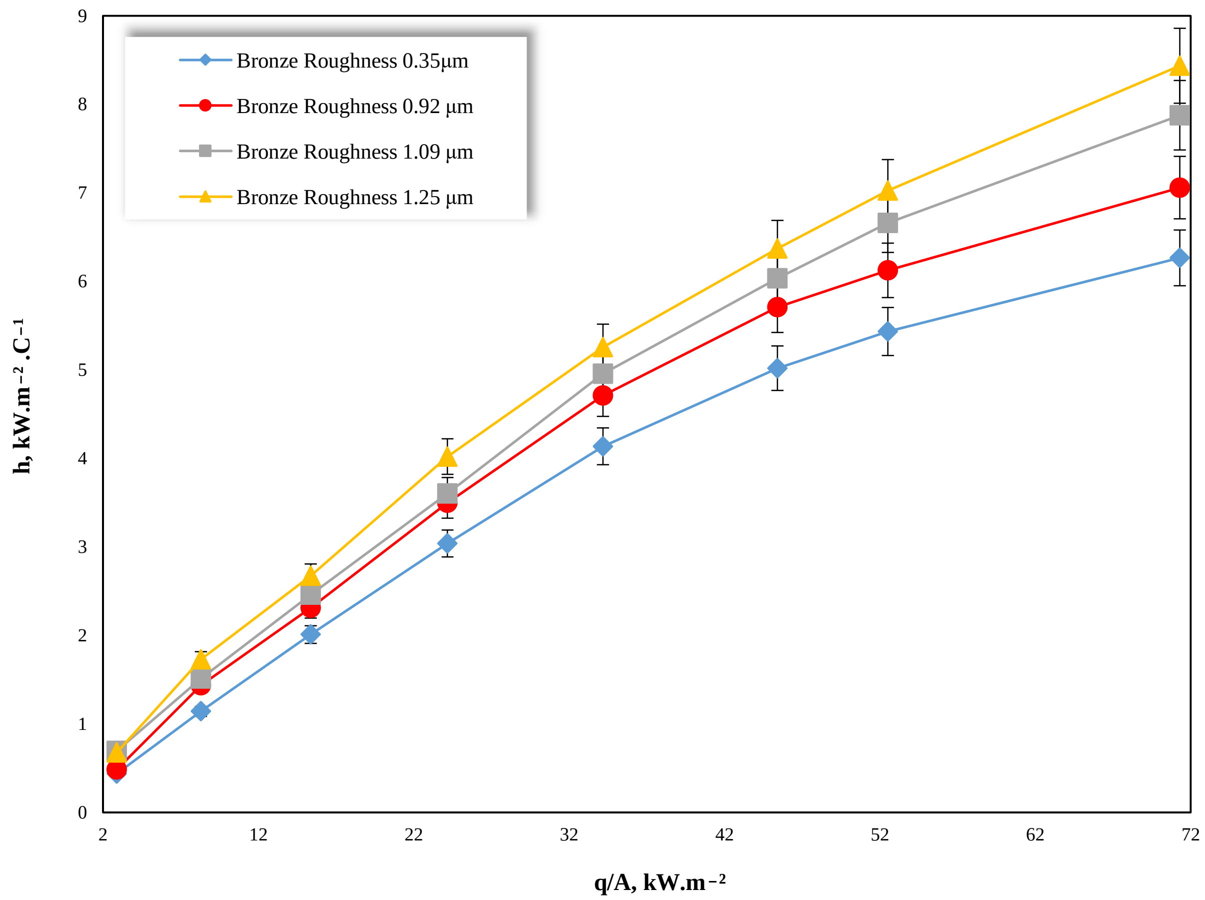

Figure 6 The effect of roughness on the BHTC

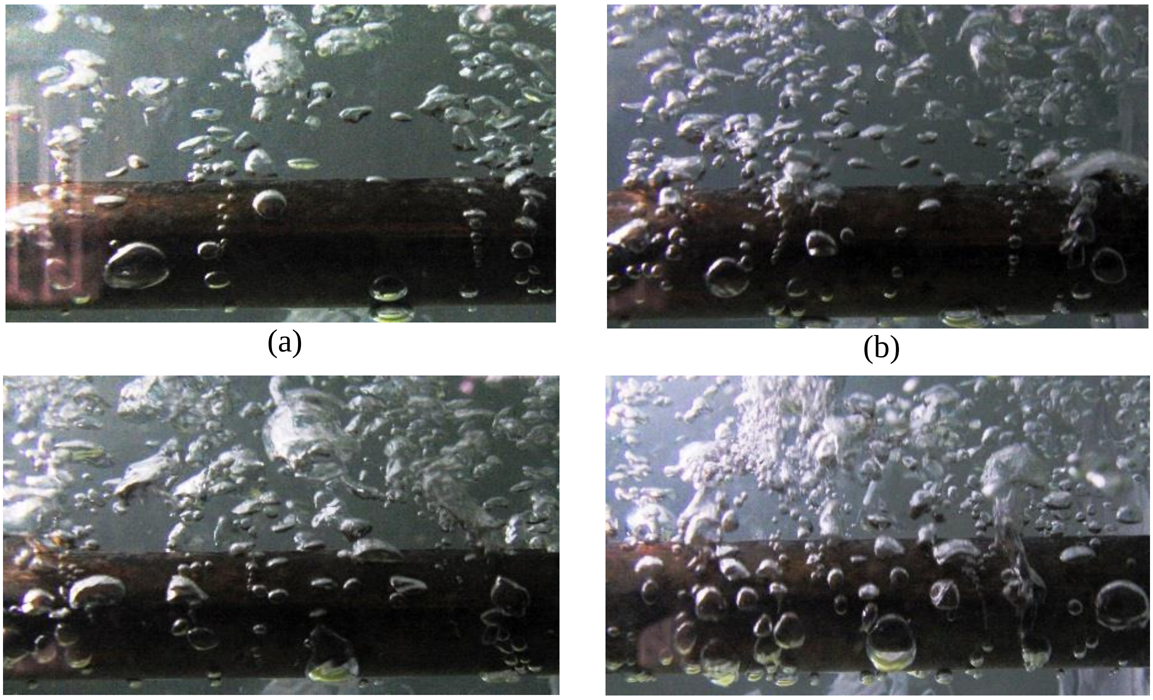

(a) (b) (c) (d)

Figure 7 The dynamic variation of the bubble through different roughnessses, a) 0.35 µm, b) 0.92 µm, c) 1.09 µm d) 1.25 µm.

5.2 Modeling and optimization of the experimental data

Due to many complex mathematical models for prediction of bubble departure diameter (Table (1)), it was necessary to find some models that were simple, easy to calculate and fast response with high accuracy. Therefore, in this work, first the experimental data were processed through powerful numerical methods of ANN and GA and Second, the opproperiate and optimized models were compared to mathematical models that were close to the experimental conditions, such as Cole[46], Van Stralen[47], Stephane[72], and Lee[52]. It should be noted that the roughness index as an independent variable and effective was considered with other variables thatweremensioned above.

5.2.1 ANN and GA approaches

An exact estimation of the examing process can have a prominent role in reducing time and cost. The authoritative tool of the artificial intelligence forecasts the complex processes which have not been introduced by specified mathematical models. In this work, the ANN was employed for modeling of the experimental data according to Table (3). Itselects the number of inputs and outputs as neurons of the input and output layers, respectively, while trial-and-error method finds number of neurons in hidden layer. Several algorithms consist of; Levenberg-Marquart (LM), Bayesian-Regulation (BR), Scaled conjugate Gradient (SCG), Random Propagation (RP), Gradient Descent Backpropagation with Adaptive Learning Rate (GDX) and etc have been introduced in the ANN. Figure (8) illustrates the optimum algorithm and the neurons of the hidden layer. As depicted in the figure, it can be found that the LM algorithm develops the network in high precision level against the other algorithms (BR, SCG, RP and GDX). Absolute average deviation (AAD) indexwith a minimum value close to zero, determined the LM algorithm by 12 neurons as the best. Concerning to the figure, it can be seen the BR is also good algorithm due to the AAD, but the LM has higher accuracy and shorter time in predicting of the experimental data. In addition, the SCG, RP and GDX had weak performances that have shown in the figure. Finally, the LM algorithm, feed-forward back propagation type and optimum architecture (10-12-1) were achieved by the optimization of the network which is demonstrated in Figure (9). The ANN produces the proper weights and biases and uses in Equation (8) which arereports in Table (4). “tansig” and “purelin” used as transfer functions of the hidden and output layers, respectively.

Moreover, forfurther investigation, the system of two hidden layers was examined. After optimization process, a structure of 10-2-11-1 by the LM algorithm was attained. The results showed that although two hidden layers had a better performance than one layer, it was complex and time-consuming with excess calculations. In this case, overfitting may be made through complicated model. Therefore, one hidden layer was choiced as general model and considered in subsequent predictions. In Table (5), numerical results are reported in terms of indicators of the absolute average deviation (AAD), the average relative deviation (ARD) and total correlation coefficient (R^2). The indices are presented as follows:

$$\mathrm{AAD} = \frac{1}{\mathrm{N}}\sum_{\mathrm{i=1}}^{\mathrm{N}}\left(\frac{y_{\mathrm{exp,i}}-y_{\mathrm{model,i}}}{y_{\mathrm{exp,i}}}\right)^2 \tag{10}$$

$$ARD = \frac{1}{\mathrm{N}}\sum_{\mathrm{i=1}}^{\mathrm{N}}\left(\frac{|y_{\mathrm{exp,i}}-y_{\mathrm{model,i}}|}{y_{\mathrm{exp,i}}}\right) \tag{11}$$

$$R^2 = \frac{\sum_{i=1}^{N}(y_{\mathrm{exp,i}}-y_{\mathrm{model,mean}})^2 - \sum_{i=1}^{N}(y_{\mathrm{exp,i}}-y_{\mathrm{model,i}})^2}{\sum_{i=1}^{N}(y_{\mathrm{model,mean}}-y_{\mathrm{exp,i}})^2} \tag{12}$$

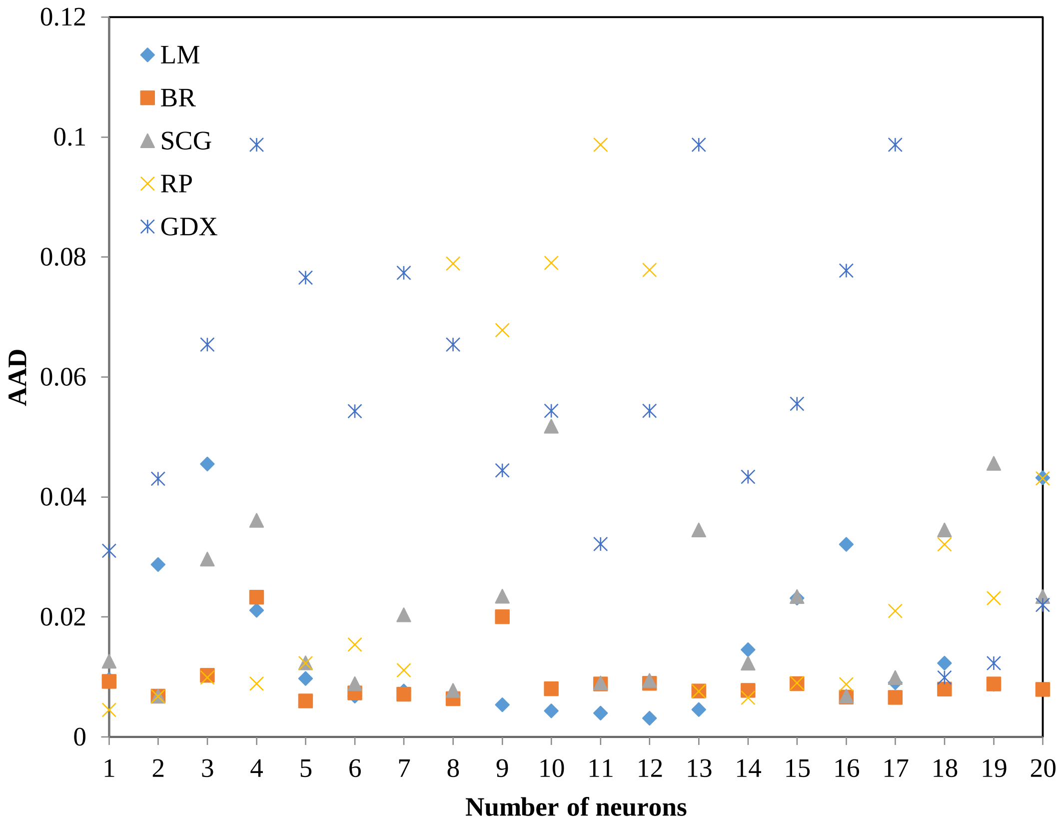

Figure 8 The optimization of the algorithm and neurons

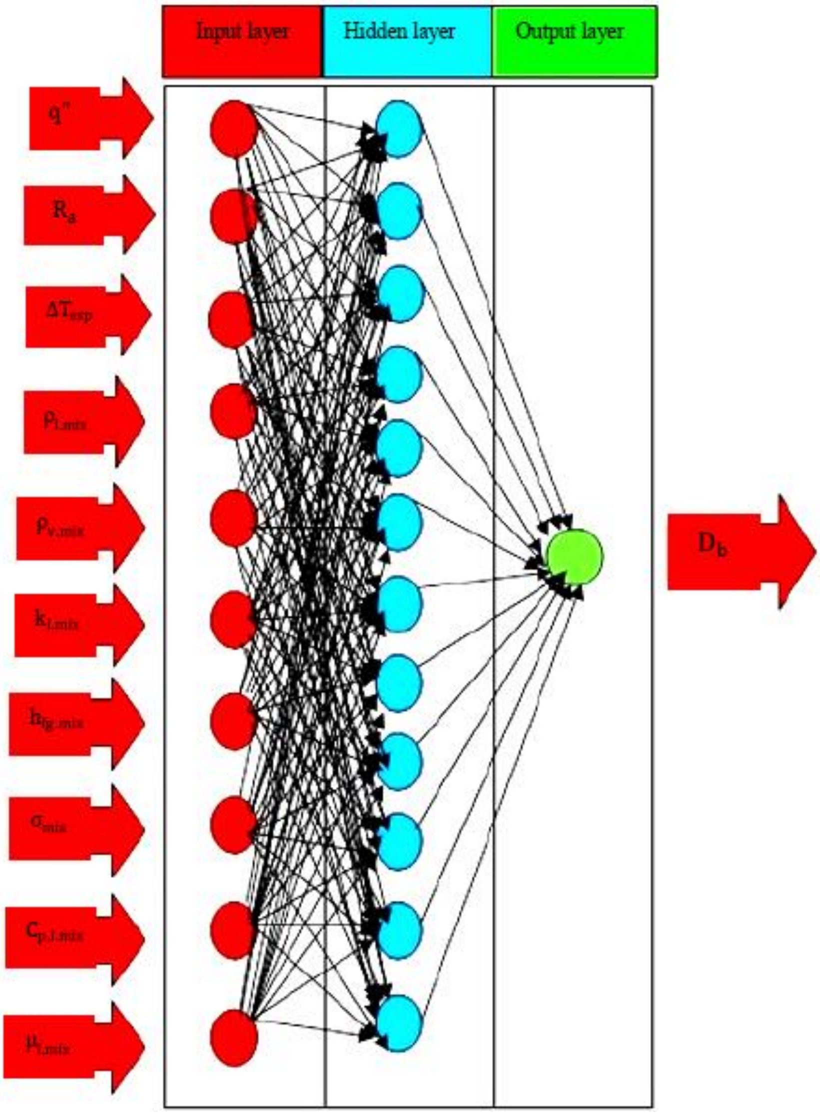

Figure 9 The optimum architecture of the processed ANN

Table 4 Proper weights and biases

Neuron	W_1										b_1	$b_2 = -0.2855$
	q''	R_a	ΔT_{exp}	$\rho_{l.mix}$	$\rho_{v.mix}$	$k_{l.mix}$	$h_{fg.mix}$	σ_{mix}	$C_{pl.mix}$	$\mu_{l.mix}$		W_2
1	-1.0284	0.9484	0.4604	0.4991	-0.5285	-0.5137	0.01259	-0.08870	0.22178	0.090	-1.7964	0.3247
2	-0.4416	-0.6803	-0.5948	-0.2745	0.7358	-0.4767	0.5847	0.4455	-0.02238	0.5731	-1.5616	0.6249
3	0.6377	0.7528	-0.3447	-0.0223	0.7995	-0.1230	-0.9771	-0.6454	-0.0743	0.0035	-1.1029	0.9179
4	-0.3713	0.5309	-0.6593	-0.3027	-0.119	-0.7115	-1.0135	0.2653	0.0009	-0.3865	0.6751	1.050
5	0.2811	0.6065	-0.5265	-0.7144	-0.0088	-0.6526	-0.5563	-0.5292	-0.3133	-0.7679	0.3827	-0.3452
6	-0.2838	-0.6138	0.8952	0.5655	-0.3629	0.9085	0.2520	-0.3065	0.0624	0.7224	0.2633	-0.6679
7	0.4374	0.1628	0.1605	-0.6139	0.8756	0.7665	0.5528	0.3492	-0.0873	0.2064	0.2456	0.3604
8	-1.2063	0.4519	0.2045	-0.7581	-0.3123	0.1572	0.3211	0.6309	0.7586	0.2985	0.6051	-0.3217
9	-0.0186	0.3892	-0.7534	-0.4285	-0.6638	-0.8779	-0.0368	-0.7217	0.4921	0.2221	-0.6843	-0.3010
10	-1.188	-0.4043	0.7259	-0.1007	0.6865	-0.722	0.1739	0.9676	0.2194	-0.4354	1.3777	0.5845
11	0.3373	-0.0913	0.7090	0.8334	-0.2246	-0.7782	-0.7725	-0.7727	0.2562	-0.499	1.5698	0.9409
12	0.7199	0.04944	-0.7094	-0.8979	-0.6344	0.1625	-0.6897	0.1828	0.2775	0.4392	1.8664	0.0741

Table 5 The performance indices of the selected ANN structures

Structure	AAD	ARD	R^2
10-12-1	0.003101	0.07610	0.9982
10-2-11-1	0.002165	0.05432	0.9988

Finally, appling GA optimizer novel correlations were determined to predict the bubble departure diameter based on power-law correlations (Eq. 9). The ranges of experimental data were used according to Table (3). Afterwards optimizing process, the correlation constants were found due to the AAD of 0.01276 and R^2 of 0.9929. The following equation introduces the power-law correlations.

$$D_b = q''^{\,0.04} * R_a^{-0.109} * \Delta T_{exp}^{\;0.361} * \rho_{l.mix}^{\;0.009} * \rho_{v.mix}^{\;10.417} * k_{l.mix}^{\;26.968} * h_{fg.mix}^{\;0.055} \cdot \sigma_{mix}^{\;0.348} * C_{pl.mix}^{\;0.215} * \mu_{l.mix}^{\;0.422} \quad (13)$$

5.2.2 Comparison of the ANN and GA with other models

The processed models were compared to Cole[46], Van Stralen[47], Stephane[72], and Lee[52]. Earlier the results revealed that the bubble diamter outputs were well forecasted by the ANN model. Figure (10) demonstrates thevalidationof the models. In this figure, it can be seen that the ANN predicts the bubble diameter data better than the GA. As depicted in Figure (10), the Cole model has a weak performance against the ANN and GA. Subsequently, the Van Stralen, Lee and Stephane models are ranked in terms of predictive power, respectively. These three models have not a good agreement with the experimental data.

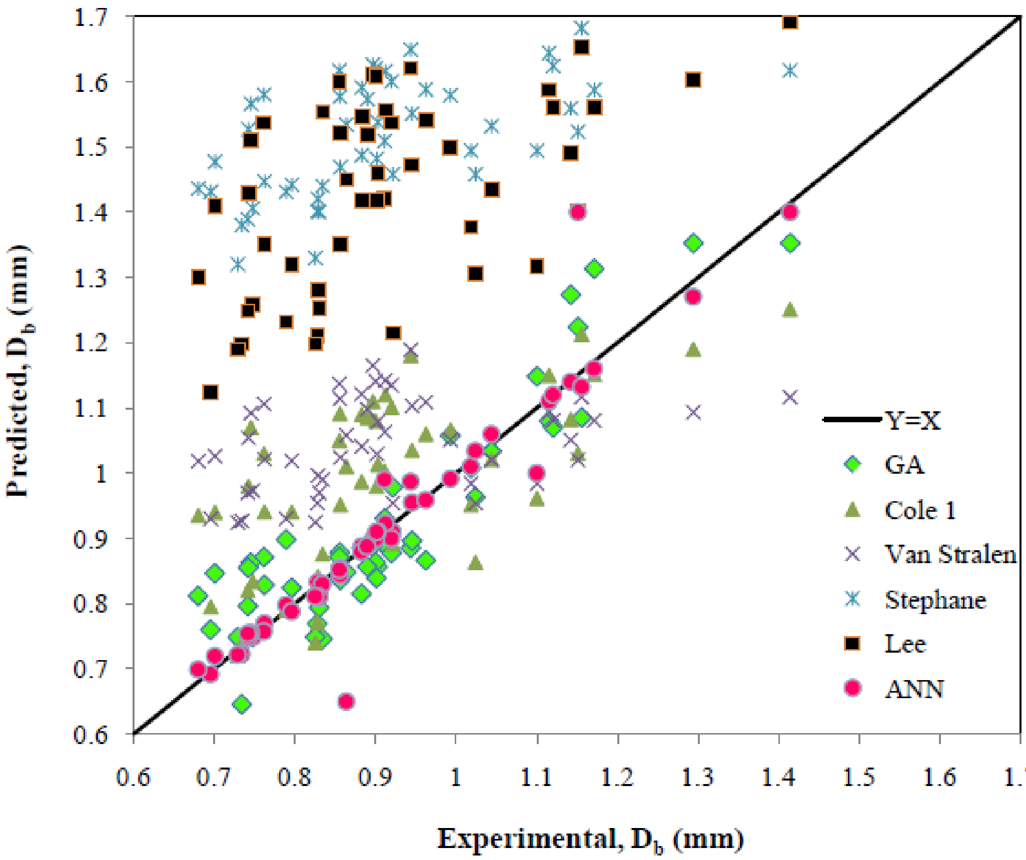

Figure 10 The comparison and validation of the proposed models

Figure (11) shows the bubble diameter versus heat flux at roughness index of 32µm. As can be observed in the figure, the ANN model is the greatest model. The GA model has also acceptable error. On the other hand, Figure (12) verifies the power of the ANN and GA in developing the measured data compared to other models. As an evaluation, this figure illustrates the variations of the bubble diameter versus the roughness index at heat flux of 71300 W.m^{-2}.
However, the ANN acts as a comprehensive information box so that the bubble departure diameteris extracted by entering the input variables. Although the GA model caused to the higher error in prediction of the buuble departure diameter than ANN, it had no vagueness, especially in introducing a clear model.

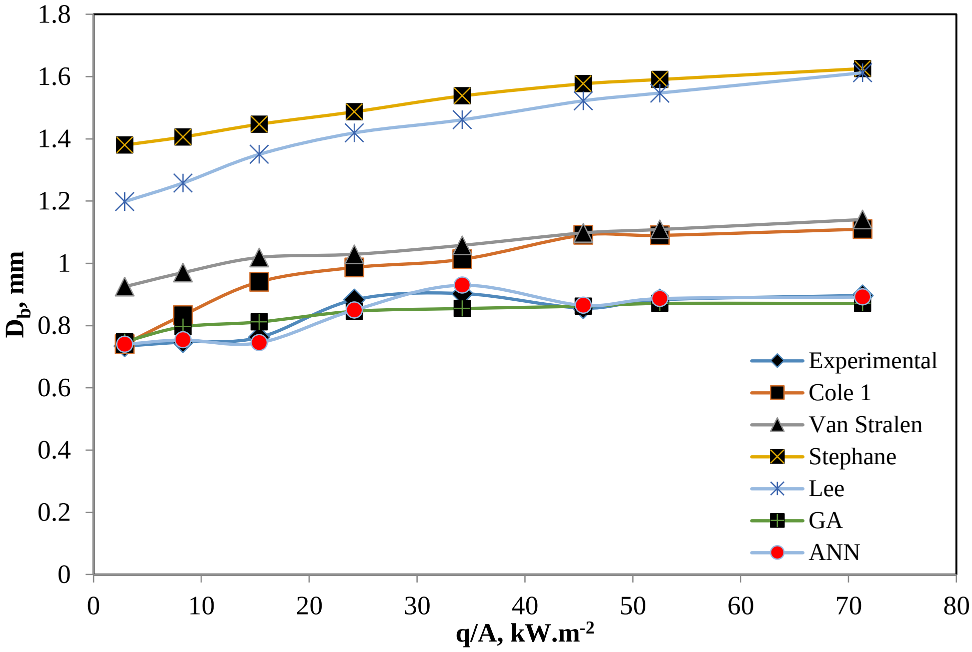

Figure 11 An evaluation of suggested models at roughness index of 32µm

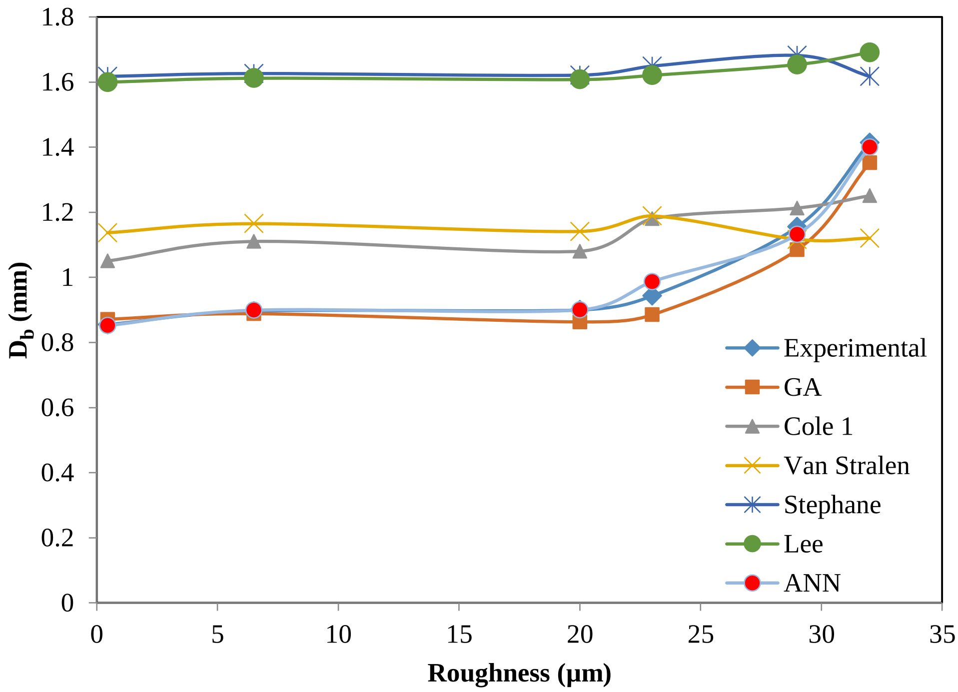

Figure 12 An evaluation of suggested models at heat flux of 71300 W.m-2

6 Conclusions

In the present work, it was attempted to study the effects of the bronze surface's roughness on thebubble departure's diameter and subsequently the heat transfer coefficent in thepool boiling. The results revealed that the roughness index was effective on the bubble dynamic. Increasing the surface roughness led to promote the bubble generation points and bubble departure diameter. Therefore,they could make a fluctuated situation and subseuently an increase in heat transferwas attained.In order to prevent errors in calculating the bubble departure's diameter due to past conventional models[46, 47, 52, 72], high-speed numerical models of artificial intelligence were processes. The ANN and GA approaches played significant roles in reducing the time and cost of experiments. These methods had superior agreement against the experimental data and also the conventional models confirmed the both models. Although the ANN showed a better performance than the GA method, the both techniques were accurate and reliable to predict the bubble departure's diameter in the pool boiling. As a conclusion, these models can be used as general models in pool boiling processes and related ones.

References

[1] J. S. Kim, A. Girard, S. Jun, J. Lee, and S. M. You, "Effect of Surface Roughness on Pool Boiling Heat Transfer of Water on Hydrophobic Surfaces," *International Journal of Heat and Mass Transfer,* vol. 118, pp. 802-811, 2018/03/01/ 2018, https://doi.org/10.1016/j.ijheatmasstransfer.2017.10.124.

[2] H. M. Ali and W. Arshad, "Effect of Channel Angle of Pin-fin Heat Sink on Heat Transfer Performance Using Water Based Graphene Nanoplatelets Nanofluids," *International Journal of Heat and Mass Transfer,* vol. 106, pp. 465-472, 2017/03/01/ 2017, https://doi.org/10.1016/j.ijheatmasstransfer.2016.08.061.

[3] M. Khooshechin, S. Fathi, F. Salimi, and S. Ovaysi, "The Influence of Surfactant and Ultrasonic Processing on Improvement of Stability and Heat Transfer Coefficient of CuO Nanoparticles in the Pool Boiling," *International Journal of Heat and Mass Transfer,* vol. 154, p. 119783, 2020/06/01/ 2020, https://doi.org/10.1016/j.ijheatmasstransfer.2020.119783.

[4] W. Arshad and H. M. Ali, "Experimental Investigation of Heat Transfer and Pressure Drop in a Straight Minichannel Heat Sink Using TiO2 Nanofluid," *International Journal of Heat and Mass Transfer,* vol. 110, pp. 248-256, 2017/07/01/ 2017, https://doi.org/10.1016/j.ijheatmasstransfer.2017.03.032.

[5] M. Khooshehchin, A. Mohammadidoust, and S. Ghotbinasab, "An Optimization Study on Heat Transfer of Pool Boiling Exposed Ultrasonic Waves and Particles Addition," *International Communications in Heat and Mass Transfer,* vol. 114, p. 104558, 2020/05/01/ 2020, https://doi.org/10.1016/j.icheatmasstransfer.2020.104558.

[6] A. Pare and S. K. Ghosh, "The Empirical Characteristics on Transient Nature of Al2O3-Water Nanofluid Pool Boiling," *Applied Thermal Engineering,* vol. 199, p. 117617, 2021/11/25/ 2021, https://doi.org/10.1016/j.applthermaleng.2021.117617.

[7] R. A. Khalaf-Allah, E. I. Eid, and A. A. Al-Nagdy, "Nucleate Pool Boiling Enhancement with the Application of a Hybrid Technique Involving the Addition of Alumina

Nanoparticles to Stirred Water above Heating Surface," *International Journal of Thermal Sciences*, vol. 170, p. 107134, 2021/12/01/ 2021, https://doi.org/10.1016/j.ijthermalsci.2021.107134.

[8] H. Peng, G. Ding, and H. Hu, "Effect of Surfactant Additives on Nucleate Pool Boiling Heat Transfer of Refrigerant-Based Nanofluid," *Experimental Thermal and Fluid Science*, vol. 35, no. 6, pp. 960-970, 2011/09/01/ 2011, https://doi.org/10.1016/j.expthermflusci.2011.01.016.

[9] H. M. Ali, M. M. Generous, F. Ahmad, and M. Irfan, "Experimental Investigation of Nucleate Pool Boiling Heat Transfer Enhancement of TiO2-water Based Nanofluids," *Applied Thermal Engineering*, vol. 113, pp. 1146-1151, 2017/02/25/ 2017, https://doi.org/10.1016/j.applthermaleng.2016.11.127.

[10] S. M. You, J. H. Kim, and K. H. Kim, "Effect of Nanoparticles on Critical Heat Flux of Water in Pool Boiling Heat Transfer," *Applied Physics Letters*, vol. 83, no. 16, pp. 3374-3376, 2003, https://doi.org/10.1063/1.1619206.

[11] P. Vassallo, R. Kumar, and S. D'Amico, "Pool Boiling Heat Transfer Experiments in Silica–water Nano-fluids," *International Journal of Heat and Mass Transfer*, vol. 47, no. 2, pp. 407-411, 2004/01/01/ 2004, https://doi.org/10.1016/S0017-9310(03)00361-2.

[12] J. Mitrovic and F. Hartmann, "A New Microstructure for Pool Boiling," *Superlattices and Microstructures*, vol. 35, no. 3, pp. 617-628, 2004/03/01/ 2004, https://doi.org/10.1016/j.spmi.2003.10.005.

[13] G. Liang and I. Mudawar, "Review of Pool Boiling Enhancement by Surface Modification," *International Journal of Heat and Mass Transfer*, vol. 128, pp. 892-933, 2019/01/01/ 2019, https://doi.org/10.1016/j.ijheatmasstransfer.2018.09.026.

[14] J. Zhou, Y. Zhang, and J. Wei, "A Modified Bubble Dynamics Model for Predicting Bubble Departure Diameter on Micro-pin-finned Surfaces under Microgravity," *Applied Thermal Engineering*, vol. 132, pp. 450-462, 2018/03/05/ 2018, https://doi.org/10.1016/j.applthermaleng.2017.12.113.

[15] H. Tang *et al.*, "Fabrication and Pool Boiling Performance Assessment of Microgroove Array Surfaces with Secondary Micro-structures for High Power Applications," *Renewable Energy*, vol. 187, pp. 790-800, 2022/03/01/ 2022, https://doi.org/10.1016/j.renene.2022.01.115.

[16] J. Y. Ho, K. K. Wong, and K. C. Leong, "Saturated Pool Boiling of FC-72 from Enhanced Surfaces Produced by Selective Laser Melting," *International Journal of Heat and Mass Transfer*, vol. 99, pp. 107-121, 2016/08/01/ 2016, https://doi.org/10.1016/j.ijheatmasstransfer.2016.03.073.

[17] D. S. Wen and B. X. Wang, "Effects of Surface Wettability on Nucleate Pool Boiling Heat Transfer for Surfactant Solutions," *International Journal of Heat and Mass Transfer*, vol. 45, no. 8, pp. 1739-1747, 2002/04/01/ 2002, https://doi.org/10.1016/S0017-9310(01)00251-4.

[18] S. K. Das, N. Putra, and W. Roetzel, "Pool Boiling Characteristics of Nano-fluids," *International Journal of Heat and Mass Transfer*, vol. 46, no. 5, pp. 851-862, 2003/02/01/ 2003, https://doi.org/10.1016/S0017-9310(02)00348-4.

[19] G. P. Narayan, K. B. Anoop, and S. K. Das, "Mechanism of Enhancement/Deterioration of Boiling Heat Transfer Using Stable Nanoparticle Suspensions Over Vertical Tubes," *Journal of Applied Physics,* vol. 102, no. 7, p. 074317, 2007, 10.1063/1.2794731.

[20] X.-Q. Wang and A. S. Mujumdar, "Heat Transfer Characteristics of Nanofluids: A Review," *International Journal of Thermal Sciences,* vol. 46, no. 1, pp. 1-19, 2007/01/01/ 2007, https://doi.org/10.1016/j.ijthermalsci.2006.06.010.

[21] M. J. Uddin, K. S. Al Kalbani, M. M. Rahman, M. S. Alam, N. Al-Salti, and I. Eltayeb, "Fundamentals of Nanofluids: Evolution, Applications and New Theory, International Journal of Biomathematics and Systems Biology," *International Journal of Biomathematics and Systems Biology,* vol. 2, no. 1, pp. 1-32, 2016.

[22] L. Lin and M. A. Kedzierski, "Review of Low-GWP Refrigerant Pool Boiling Heat Transfer on Enhanced Surfaces," *International Journal of Heat and Mass Transfer,* vol. 131, pp. 1279-1303, 2019/03/01/ 2019, https://doi.org/10.1016/j.ijheatmasstransfer.2018.11.142.

[23] N. K. Choon, A. Chakraborty, S. M. Aye, and W. Xiaolin, "New Pool Boiling Data for Water with Copper-foam Metal at Sub-atmospheric Pressures: Experiments and Correlation," *Applied Thermal Engineering,* vol. 26, no. 11, pp. 1286-1290, 2006/08/01/ 2006, https://doi.org/10.1016/j.applthermaleng.2005.10.028.

[24] A. Jaikumar and S. G. Kandlikar, "Enhanced Pool Boiling for Electronics Cooling Using Porous Fin Tops on Open Microchannels with FC-87," *Applied Thermal Engineering,* vol. 91, pp. 426-433, 2015/12/05/ 2015, https://doi.org/10.1016/j.applthermaleng.2015.08.043.

[25] Z. G. Xu and C. Y. Zhao, "Influences of Nanoparticles on Pool Boiling Heat Transfer in Porous Metals," *Applied Thermal Engineering,* vol. 65, no. 1, pp. 34-41, 2014/04/01/ 2014, https://doi.org/10.1016/j.applthermaleng.2013.12.077.

[26] N. Rykalin and V. Kudinov, "Plasma Spraying," in *Plasma Chemistry–2: Plasma Chemistry and Transport Phenomena in Thermal Plasmas*: Elsevier, 1976, pp. 229-239.

[27] M. Jakob, "Heat Transfer pp. 636-638," ed: John Wiley & Sons, New York, 1949.

[28] C.-D. Wen and I. Mudawar, "Emissivity Characteristics of Roughened Aluminum Alloy Surfaces and Assessment of Multispectral Radiation Thermometry (MRT) Emissivity Models," *International Journal of Heat and Mass Transfer,* vol. 47, no. 17, pp. 3591-3605, 2004/08/01/ 2004, https://doi.org/10.1016/j.ijheatmasstransfer.2004.04.025.

[29] P. J. Marto and W. M. Rohsenow, "Effects of Surface Conditions on Nucleate Pool Boiling of Sodium," *Journal of Heat Transfer,* vol. 88, no. 2, pp. 196-203, 1966.

[30] T. S. Emery, A. Jaikumar, P. Raghupathi, I. Joshi, and S. G. Kandlikar, "Dual Enhancement in HTC and CHF for External Tubular Pool Boiling – A Mechanistic Perspective and Future Directions," *International Journal of Heat and Mass Transfer,* vol. 122, pp. 1053-1073, 2018/07/01/ 2018, https://doi.org/10.1016/j.ijheatmasstransfer.2018.01.138.

[31] M. Hassanpour, B. Vaferi, and M. E. Masoumi, "Estimation of Pool Boiling Heat Transfer Coefficient of Alumina Water-based Nanofluids by Various Artificial Intelligence

(AI) approaches," *Applied Thermal Engineering*, vol. 128, pp. 1208-1222, 2018/01/05/ 2018, https://doi.org/10.1016/j.applthermaleng.2017.09.066.

[32] S. K. Roy Chowdhury and R. H. S. Winterton, "Surface Effects in Pool Boiling," *International Journal of Heat and Mass Transfer*, vol. 28, no. 10, pp. 1881-1889, 1985/10/01/ 1985, https://doi.org/10.1016/0017-9310(85)90210-8.

[33] S. T. Hsu and F. W. Schmidt, "Measured Variations in Local Surface Temperatures in Pool Boiling of Water," *Journal of Heat Transfer*, vol. 83, no. 3, pp. 254-260, 1961, https://doi.org/10.1115/1.3682252.

[34] P. J. Berenson, "Experiments on Pool-boiling Heat transfer," *International Journal of Heat and Mass Transfer*, vol. 5, no. 10, pp. 985-999, 1962/10/01/ 1962, https://doi.org/10.1016/0017-9310(62)90079-0.

[35] J. M. S. Jabardo, G. Ribatski, and E. Stelute, "Roughness and Surface Material Effects on Nucleate Boiling Heat Transfer from Cylindrical Surfaces to Refrigerants R-134a and R-123," *Experimental Thermal and Fluid Science*, vol. 33, no. 4, pp. 579-590, 2009/04/01/ 2009, https://doi.org/10.1016/j.expthermflusci.2008.12.004.

[36] K. K. Wong and K. C. Leong, "Saturated Pool Boiling Enhancement Using Porous Lattice Structures Produced by Selective Laser Melting," *International Journal of Heat and Mass Transfer*, vol. 121, pp. 46-63, 2018/06/01/ 2018, https://doi.org/10.1016/j.ijheatmasstransfer.2017.12.148.

[37] S. A. Alavi Fazel, "A Genetic Algorithm-based Optimization Model for Pool Boiling Heat Transfer on Horizontal Rod Heaters at Isolated BubbleRegime," *Heat and Mass Transfer*, vol. 53, no. 9, pp. 2731-2744, 2017/09/01 2017, https://doi.org/10.1007/s00231-017-2013-8.

[38] M.-G. Kang, "Effect of Surface Roughness on Pool Boiling Heat Transfer," *International Journal of Heat and Mass Transfer*, vol. 43, no. 22, pp. 4073-4085, 2000/11/15/ 2000, https://doi.org/10.1016/S0017-9310(00)00043-0.

[39] G. Ribatski and J. M. S. Jabardo, "Experimental Study of Nucleate Boiling of Halocarbon Refrigerants on Cylindrical Surfaces," *International Journal of Heat and Mass Transfer*, vol. 46, no. 23, pp. 4439-4451, 2003/11/01/ 2003, https://doi.org/10.1016/S0017-9310(03)00252-7.

[40] V. Tolubinskii, "Heat Exchange During Boiling," *Kiev Izdatel Naukova Dumka*, 1980.

[41] I. L. Pioro, W. Rohsenow, and S. S. Doerffer, "Nucleate Pool-boiling Heat Transfer. I: Review of Parametric Effects of Boiling Surface," *International Journal of Heat and Mass Transfer*, vol. 47, no. 23, pp. 5033-5044, 2004/11/01/ 2004, https://doi.org/10.1016/j.ijheatmasstransfer.2004.06.019.

[42] C. Gerardi, J. Buongiorno, L.-w. Hu, and T. McKrell, "Study of Bubble Growth in Water Pool Boiling Through Synchronized, Infrared Thermometry and High-speed Video," *International Journal of Heat and Mass Transfer*, vol. 53, no. 19, pp. 4185-4192, 2010/09/01/ 2010, https://doi.org/10.1016/j.ijheatmasstransfer.2010.05.041.

[43] J. F. Klausner, R. Mei, D. M. Bernhard, and L. Z. Zeng, "Vapor Bubble Departure in Forced Convection Boiling," *International Journal of Heat and Mass Transfer*, vol. 36, no. 3, pp. 651-662, 1993/02/01/ 1993, https://doi.org/10.1016/0017-9310(93)80041-R.

[44] W. Fritz, "Berechnung des Maximalvolumes von Dampfblasen," *Physik. Zeitschr*, vol. 36, pp. 379-384, 1935 1935. [Online]. Available: https://cir.nii.ac.jp/crid/1573668924962839808.

[45] R. Ruckenstein, "Recent Trends in Boiling Heat Transfer Research," *Appl. Mech. Rev*, vol. 17, pp. 663-672, 1964.

[46] R. Cole, "Bubble Frequencies and Departure Volumes at Subatmospheric Pressures," *AIChE Journal*, vol. 13, no. 4, pp. 779-783, 1967/07/01 1967, https://doi.org/10.1002/aic.690130434.

[47] S. J. D. Van Stralen and W. Zijl, "Fundamental Developments in Bubble Dynamics," 1978: Begel House Inc.

[48] S. S. Kutateladze and Gogonin, II, "Growth Rate and Detachment Diameter of a Vapor Bubble in Free Convection Boiling of a Saturated Liquid," *Teplofizika Vysokikh Temperatur*, vol. 17, pp. 792-797, 1979.

[49] G. Kocamustafaogullari, "Pressure Dependence of Bubble Departure Diameter for Water," *International Communications in Heat and Mass Transfer*, vol. 10, no. 6, pp. 501-509, 1983/11/01/ 1983, https://doi.org/10.1016/0735-1933(83)90057-X.

[50] M. K. Jensen and G. J. Memmel, "Evaluation of Bubble Departure Diameter Correlations," 1986: Begel House Inc.

[51] D. Gorenflo, V. Knabe, and V. Bieling, "Bubble Density on Surfaces with Nucleate Boiling-its Influence on Heat Transfer and Burnout Heat Flux at Elevated Saturation Pressures," 1986: Begel House Inc.

[52] H. C. Lee, B. D. Oh, S. W. Bae, and M. H. Kim, "Single Bubble Growth in Saturated Pool Boiling on a Constant Wall Temperature Surface," *International Journal of Multiphase Flow*, vol. 29, no. 12, pp. 1857-1874, 2003/12/01/ 2003, https://doi.org/10.1016/j.ijmultiphaseflow.2003.09.003.

[53] G. Sateesh, S. K. Das, and A. R. Balakrishnan, "Analysis of Pool Boiling Heat Transfer: Effect of Bubbles Sliding on the Heating Surface," *International Journal of Heat and Mass Transfer*, vol. 48, no. 8, pp. 1543-1553, 2005.

[54] H. T. Phan, N. Caney, P. Marty, S. Colasson, and J. Gavillet, "Surface Wettability Control by Nanocoating: The Effects on Pool Boiling Heat Transfer and Nucleation Mechanism," *International Journal of Heat and Mass Transfer*, vol. 52, no. 23, pp. 5459-5471, 2009/11/01/ 2009, https://doi.org/10.1016/j.ijheatmasstransfer.2009.06.032.

[55] S. A. Alavi Fazel and S. B. Shafaee, "Bubble Dynamics for Nucleate Pool Boiling of Electrolyte Solutions," *Journal of Heat Transfer*, vol. 132, no. 8, 2010, 10.1115/1.4001315.

[56] H. T. Phan, N. Caney, P. Marty, S. Colasson, and J. Gavillet, "A Model to Predict the Effect of Contact Angle on the Bubble Departure Diameter During Heterogeneous Boiling," *International Communications in Heat and Mass Transfer,* vol. 37, no. 8, pp. 964-969, 2010.

[57] S. Van Stralen and W. Zijl, "Fundamental Developments in Bubble Dynamics," in *International Heat Transfer Conference Digital Library*, 1978: Begel House Inc.

[58] S. Kutateladze and I. Gogonin, "Growth Rate and Detachment Diameter of a Vapor Bubble in Free Convection Boiling of a Saturated Liquid," *Teplofizika Vysokikh Temperatur,* vol. 17, pp. 792-797, 1979.

[59] M. K. Jensen and G. J. Memmel, "Evaluation of Bubble Departure Diameter Correlations," in *International Heat Transfer Conference Digital Library*, 1986: Begel House Inc.

[60] D. Gorenflo, V. Knabe, and V. Bieling, "Bubble Density on Surfaces with Nucleate Boiling-Its Influence on Heat Transfer and Burnout Heat Flux at Elevated Saturation Pressures," in *International Heat Transfer Conference Digital Library*, 1986: Begel House Inc.

[61] H. C. Lee, B. Do Oh, S. W. Bae, and M. H. Kim, "Single Bubble Growth in Saturated Pool Boiling on a Constant Wall Temperature Surface," *International Journal of Multiphase Flow,* vol. 29, no. 12, pp. 1857-1874, 2003.

[62] S. A. A. Fazel and S. B. Shafaee, "Bubble Dynamics for Nucleate Pool Boiling of Electrolyte Solutions," *Journal of Heat Transfer,* vol. 132, no. 8, p. 081502, 2010.

[63] K. Stephan, "Saturated Pool Boiling and Subcooled Flow Boiling of Mixtures," Ph. D. thesis, University of Auckland, New Zealand, 1992.

[64] M. Cooper and A. Lloyd, "The Microlayer in Nucleate Pool Boiling," *International Journal of Heat and Mass Transfer,* vol. 12, no. 8, pp. 895-913, 1969.

[65] B. E. Staniszewski, "Nucleate Boiling Bubble Growth and Departure," Cambridge, Mass.: Massachusetts Institute of Technology, 1959, Division of Industrial Cooperation.

[66] N. Zuber, "Nucleate Boiling. The Region of Isolated Bubbles and the Similarity with Natural Convection," *International Journal of Heat and Mass Transfer,* vol. 6, no. 1, pp. 53-78, 1963.

[67] A. Hatton and I. Hall, "Photographic Study of Boiling on Prepared Surfaces," in *International Heat Transfer Conference Digital Library*, 1966: Begel House Inc.

[68] R. Cole and H. Shulman, "Bubble Departure Diameters at Subatmospheric Pressures," in *Chem. Eng. Prog. Symp. Ser*, 1966, vol. 62, no. 64, pp. 6-16.

[69] R. Cole and W. Rohsenow, "Correlation of Bubble Departure Diameters for Boiling of Saturated Liquids," in *Chem. Eng. Prog. Symp. Ser,* 1969, vol. 65, no. 92: 211 213, pp. 211-213.

[70] Y. Kweon and M. Kim, "Experimental Study on Nucleate Boiling Enhancement and Bubble Dynamic Behavior in Saturated Pool Boiling Using a Nonuniform dc Electric Field," International Journal of Multiphase Flow, vol. 26, no. 8, pp. 1351-1368, 2000.

[71] M. Jamialahmadi, A. Helalizadeh, and H. Müller-Steinhagen, "Pool Boiling Heat Transfer to Electrolyte Solutions," *International Journal of Heat and Mass Transfer*, vol. 47, no. 4, pp. 729-742, 2004.

[72] K. Stephan, "Saturated Pool Boiling and Subcooled flow Boiling of Mixtures," *University of Auckland, Newzland*, 1992.

[73] M. G. Cooper and A. J. P. Lloyd, "The Microlayer in Nucleate Pool Boiling," *International Journal of Heat and Mass Transfer*, vol. 12, no. 8, pp. 895-913, 1969/08/01/ 1969, https://doi.org/10.1016/0017-9310(69)90154-9.

[74] H. B. Demuth and M. H. Beale, *Neural Network Toolbox: for Use with MATLAB: User's Guide*. MathWorks, Incorporated, 2000.

[75] L. M. Schmitt, "Theory of Genetic Algorithms II: Models for Genetic Operators Over the String-tensor Representation of Populations and Convergence to Global Optima for Arbitrary Fitness Function Under Scaling," *Theoretical Computer Science*, vol. 310, no. 1, pp. 181-231, 2004/01/01/ 2004, https://doi.org/10.1016/S0304-3975(03)00393-1.

[76] D. E. Goldberg, "Genetic Algorithms in Search, Optimization and Machine Learning,. Addition-Westly," *Reading MA*, 1989.

Nomenclature

A	Area, m^2
Ar	Archimedes number
D	Bubble diameter, mm
f	Bubble frequency, Hz
H	Latent heat, $J.g^{-1}$
h	Heat transfer coefficient, $W.m^{-2}.C^{-1}$
Ja	Jacob number
K	Thermal conductivity coefficient
L	Length, m
M	Molecular weight
I	Current, A
$\frac{N}{A}$	Nucleation site Points
Pr	Prandtl number
q	Heat, W
R_a	Roughness average surface, μm
S	Surface
T	Temperature, C
t	Time, S
V	Voltage, V
W	Watt, W
X	Liquid mole fraction

Greek symbols

α	Thermal penetration
δ	Heat penetration depth, m
ρ	Density, $kg.m^{-3}$
μ	Viscosity, $kg.m^{-1}.s^{-1}$
σ	Surface tension, $N.m^{-1}$
π	Pi number
θ	Angle
Δ	Difference
ξ	Parameter Estimating the effect of electric field

Subscripts or superscripts

b	Bubble
c	Critical
d	Departure
f	Fluid
g	Growing
l	Liquid
sat	Saturation
v	Vapor
th	Thermometers